JOURNAL OF SOLID STATE CHEMISTRY 40, 318–329 (1981)

Crystal Chemistry, Modulated Structure, and Electrical Conductivity in the Oxygen Excess Scheelite-Based Compounds $La_{1-x}Th_xNbO_{4+x/2}$ and $LaNb_{1-x}W_xO_{4+x/2}$

R. J. CAVA

Bell Laboratories, Murray Hill, New Jersey 07974

AND R. S. ROTH, T. NEGAS, H. S. PARKER, AND D. B. MINOR

National Bureau of Standards, Washington, D.C. 20234

Received February 6, 1981; in revised form August 12, 1981

For $La_{1-x}Th_xNbO_{4+x/2}$, three phases with broad homogeneity regions occur, for $0.075 \leq x \leq 0.37$, $0.41 < x < 0.61$, and $0.65 \leq x \leq 0.74$. All are related to the scheelite structure type, with at least the first exhibiting an incommensurate structural modulation. An analogous structurally modulated phase was found for $LaNb_{1-x}W_xO_{4+x/2}$ for $0.11 \leq x \leq 0.22$. Additional phases occur at $La_{0.2}Th_{0.8}NbO_{4.4}$ and $LaNb_{0.4}W_{0.6}O_{4.3}$. The electrical conductivity and the direction and wavelength of the structural modulation have been characterized for the $La_{1-x}Th_xNbO_{4+x/2}$ phase with $0.075 \leq x \leq 0.37$.

Introduction

Studies of compounds of ceria with tantala and niobia have led to the discovery of complex low-temperature oxidation/reduction reactions in $CeTaO_4$ and $CeNbO_4$ (*1–4*). We describe here experiments on compounds with structures related to $CeNbO_4$, which has a monoclinic distortion of the scheelite ($CaWO_4$) structure type at room temperature (*5*). All other ABO_4 rare earth niobates and tantalates, excepting the La, Ce, and Pr tantalates, have the same structure type. Previous TGA, DTA, and X-ray diffraction studies (*2–4*) have indicated that the oxidation of $CeNbO_4$ leads to the formation of several new phases of approximate compositions $CeNbO_{4.08}$, $CeNbO_{4.25}$, and $CeNbO_{4.33}$. The charge is balanced on the accommodation of excess oxygen by the oxidation of some of the Ce^{3+} normally present to Ce^{4+}. The $CeNbO_{4.08}$ and $CeNbO_{4.25}$ phases have crystal structures related closely to $CeNbO_4$, but with additional ordering resulting in superlattice reflections in X-ray diffraction patterns. We show here that the $CeNbO_{4.08}$ type phase is an incommensurate modulated structure. The presence of mixed-valence cerium ions in the oxidized phase suggests the presence of hopping-type conductivity, and the rapidity of the oxidation/reduction kinetics indicates at least a high chemical diffusion coefficient for oxygen.

The detailed study of the oxygen-excess phases of $CeNbO_4$ is difficult due to their limited temperature/oxygen partial pressure stability regions. These difficulties have been overcome by introduction of excess oxygen to the isostructural compound $LaNbO_4$ by doping with $ThNbO_{4.5}$, and

0022-4596/81/150318-12$02.00/0

Copyright © 1981 by Academic Press, Inc.
All rights of reproduction in any form reserved.

$LaWO_{4.5}$, forming compounds of the type $A^{4+,3+}NbO_{4+x}$ and $LaB^{5+,6+}O_{4+x}$, where $0 \leq x \leq 0.5$. The compounds formed are stable over wide ranges of temperature and oxygen partial pressure and are, in many cases, apparently isostructural with the oxidized variants of $CeNbO_4$. The wavelength of the structural modulation for the $CeNbO_{4.08}$ type phase in the $(La,Th)NbO_{4+x}$ system is continuously variable over a wide range of oxygen excess. The electrical conductivities of the $LaNbO_4$ end-member and three compositions in the structurally modulated phase have been measured. The synthesis, crystal chemistry, and phase equilibria in the $LaNbO_4$–$LaWO_{4.5}$ and $LaNbO_4$–$ThNb_{4.5}$ systems are described, as are the characterization of the structural modulation and the electrical conductivity for the $CeNbO_{4.08}$ type phase in the $(La,Th)NbO_{4+x}$ system.

Experimental

The desired compositions were prepared from Nb_2O_5, $La(OH)_3$ (prepared from La_2O_3 by boiling in deionized water and drying at 100°C), WO_3, and $Th(NO_3)_4$. Powders were calcined in platinum tubes, which, for the tungsten-containing samples, were sealed to avoid loss of WO_3. Samples were fired in air in a furnace where temperatures were known to ±20°C for the general subsolidus studies. To determine phase boundaries and solidus temperatures more accurately, the appropriate samples were calcined in an electrically heated vertical tube furnace controlled by an ac Wheatstone bridge controller capable of holding temperatures to ±2°C for extended time periods. Temperatures were measured with a Pt–Pt/10%Rh thermocouple which had been calibrated against the melting points of Au (1063°C) and Pd (1552°C). Tungsten oxide-containing samples in sealed tubes were quenched in water to test for tube leakage, and thorium-containing samples in unsealed Pt tubes were air-quenched.

Equilibrium was considered to have been obtained when the X-ray diffraction patterns of specimens successively heated for longer times and/or at higher temperatures showed no change. Intermediate grindings were performed in an agate mortar and pestle. The first sign of glazing of the surface of the specimen was interpreted as the first experimental evidence for the solidus temperature. This was accompanied in most instances by an abrupt difference in the X-ray diffraction powder patterns of the specimens. In the few cases where we determined liquidus temperatures, the sample condition was taken as the formation of a concave meniscus without the formation of large crystals.

Dense polycrystalline pellets were employed as specimens for electrical conductivity measurements. Raw materials were prereacted at a low temperature (about 1100°C) in platinum crucibles until nearly single phase material was obtained. This generally required calcining for 1 to 2 weeks. The powders were then jet-milled to break up agglomerates. The mean particle sizes were on the order of 10 μm. Pellets were prepared by cold-pressing at 2000 psi in a steel die, with a saturated solution of stearic acid in methanol used in small amounts as a binder. Pellets were fired in air at 1350°C for 32 hr, with 6-hr heating and cooling periods. Densities for all samples were 90 ± 1% of theoretical, except for pure $LaNbO_4$, for which densities in excess of 80% of theoretical were not obtained. Measurements were made on pellets of about 1.0 cm diameter and 0.25 cm height. Surfaces were ground and polished on 600 grit silicon carbide paper. Platinum paste was applied to the flat pellet faces to serve as electrodes. Several layers of paste were applied and dried at 60°C before firing at 1000°C for 10 hr.

Conductivity measurements were made

in a tube furnace with nichrome wire heating elements laid parallel to its axis to minimize inductive effects. Temperature was read by a 100Pt–90Pt10Rh thermocouple in contact with the sample electrode. The two measurement leads were constructed to form a single coaxial cable which ran concentric with the furnace axis. Complex impedance measurements were made at frequencies between 56 Hz and 13 MHz with a commercial network analyzer. A signal generator was employed to apply a potential of 0.4 V to the sample. The sample impedance was measured by taking the differences in the response of the sample circuit and a circuit which was designed to balance as nearly as possible the impedance of the sample circuit (without sample) with an equivalent length of coaxial cable.

Phase Equilibria

$LaNbO_4$–$LaWO_{4.5}$

Seventeen compositions were prepared in the binary system $LaNbO_4$–$LaWO_{4.5}$, in general at 10 mole% intervals, and, where necessary to clarify the phase equilibria at finer intervals. Charge balance in this case is achieved in a different manner than in the $CeNbO_{4+x}$ compounds, but we nonetheless found a phase with composition and structure analogous to $CeNbO_{4.08}$. The phase equilibria diagram is shown in Fig. 1. $LaNbO_4$ has a monoclinic distortion of the scheelite structure at room temperature with $a = 5.564$, $b = 11.488$, $c = 5.196$ Å, and $\beta = 94.5°$. Very little $LaWO_{4.5}$ can be added to $LaNbO_4$ without the formation of the $CeNbO_{4.08}$ type phase: a two-phase region exists between approximately $LaNb_{0.98}W_{0.02}O_{4.01}$ and $LaNb_{0.89}W_{0.11}O_{4.055}$. Single-crystal precession photographs indicate that the average structure of the $CeNbO_{4.08}$-type phase is strongly related to that of $LaNbO_4$. However, the presence of additional Bragg peaks at incommensurate locations in reciprocal space is indicative of an additional ordering in the form of a sinusoidal structural modulation. The pres-

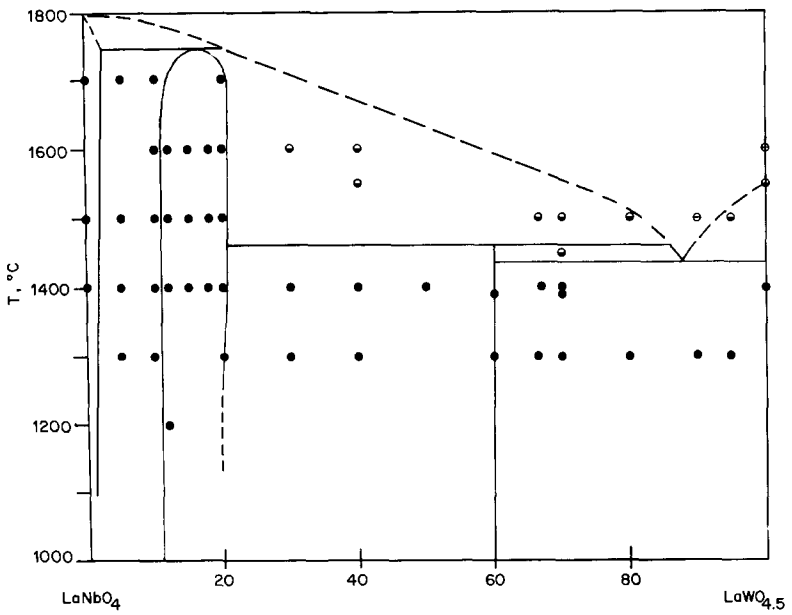

FIG. 1. Phase equilibrium diagram for the system $LaNbO_4$–$LaWO_{4.5}$. ●, no melting; ◒, partially melted; ⊖, completely melted.

ence of a two-phase region indicates that a minimum defect concentration is necessary for the formation of the structurally modulated phase, which exists between the compositions $LaNb_{0.89}W_{0.11}O_{4.055}$ and $LaNb_{0.78}W_{0.22}O_{4.11}$. No range of composition has been observed in the $CeNbO_{4.08}$ oxidized variant of $CeNbO_4$, perhaps due to the difficulty in defining the oxygen partial pressure and temperature conditions under which different compositions might be stable.

The average structure changes from being dimensionally monoclinic to dimensionally tetragonal over the range of existence of the structurally modulated phase. Near the low oxygen limit, $LaNb_{0.88}W_{0.12}O_{4.06}$, the lattice parameters estimated from five low-angle average structure reflections are, $a = 5.41, b = 11.62, c = 5.29$ Å, $\beta = 91.62$, and near the high oxygen limit, $LaNb_{0.8}W_{0.2}O_{4.1}$, they are $a = c = 5.34, b = 11.69$ ($\beta = 90°$). The parameters apparently change in a continuous manner as a function of oxygen content. The structural modulation is characterized by two additional periodicities, and is discussed in later sections.

A relatively large two-phase region exists between the oxygen-rich boundary of the modulated structure and the second intermediate compound at $LaNb_{0.4}W_{0.6}O_{4.3}$, which melts incongruently. This phase is apparently unrelated to any of the oxidized variants of $CeNbO_4$. Attempts to obtain single crystals of a size suitable for X-ray study, by annealing at temperatures below the melting point for extended periods, were not successful and we were therefore unable to index the powder diffraction pattern. The five strongest lines in the powder pattern are at $d = 4.263$, 3.221, 2.928, 2.637, and 1.984 Å. We found no evidence for the existence of a range of stoichiometry for this compound.

We observed no signs of melting for $LaNbO_4$ at temperatures up to 1760°C although the reported melting point is 1620 ± 30°C (*11*). In addition, we attempted to find the unit cell parameters for $LaWO_{4.5}$, which had been previously reported (*6*) as a compound. Small single crystals were obtained by induction melting single phase material at approximately 1650°C in air in an iridium crucible. We looked at several crystals on the precession camera but were unable to find any symmetry. Several triclinic cells were investigated for indexing based on the precession photographs. A reduced triclinic cell, $a = 7.047, b = 7.345, c = 7.104$ Å, $\alpha = 69.13$, $\beta = 85.15$, $\gamma = 83.55°$ did not index all of the Bragg reflections in the powder pattern. In addition, none of the seven cells with doubled cell volume, generated by the program of Santoro and Mighell (*7*) were able to index the powder pattern. The five strongest lines in the pattern were at 3.418, 3.233, 3.124, 3.052, and 3.008 Å. Preparation of several compositions in the La_2O_3–WO_3 binary system near the $La_2O_3 : 2WO_3$ composition indicated that the phase was indeed at $LaWO_{4.5}$, as previously reported. The true unit cell and symmetry of this phase remain in doubt.

$LaNbO_4$–$ThNbO_{4.5}$

Twenty-seven compositions were prepared in the binary system $LaNbO_4$–$ThNbO_{4.5}$. Charge balance in this case is achieved in a manner equivalent to that in $CeNbO_{4.08}$. Four intermediate ranges of compounds were found, necessitating the preparation of a large number of compositions to clarify the phase equilibria. The phase equilibria diagram is shown in Fig. 2. Up to about 3% thorium can be substituted for lanthanum in $LaNbO_4$ before the defect $CeNbO_{4.08}$-type phase begins to form. A two-phase region exists between approximately $La_{0.97}Th_{0.03}NbO_{4.015}$ and $La_{0.925}Th_{0.075}NbO_{4.0375}$. The minimum defect concentration necessary for the formation of the incommensurate, structurally modulated phase in this system is lower than in

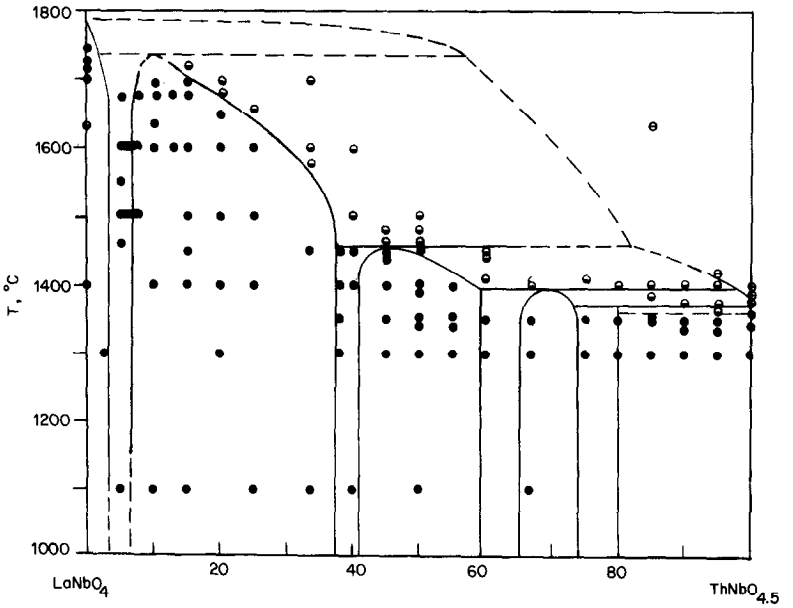

FIG. 2. Phase equilibrium diagram for the system $LaNbO_4$–$ThTaO_{4.5}$. ●, no melting; ◒, partially melted; ⊖, completely melted.

the $LaNbO_4$–$LaWO_{4.5}$ system. This phase, which is exactly analogous to $CeNbO_{4.08}$, exists over a wide range of oxygen excess, between the compositions $La_{0.925}Th_{0.075}NbO_{4.0375}$ and $La_{0.63}Th_{0.37}NbO_{4.185}$.

The subcell (average structure) parameters of pure $LaNbO_4$ and the structurally modulated phase were estimated from five low-angle lines observed in X-ray powder diffraction patterns. All cell parameters display a discontinuous change at the $LaNbO_4$-modulated phase boundary, indicating that change is first order in composition. Within experimental error, b and c increase slightly in the modulated phase, and a decreases in a continuous manner until it becomes equal to c at about $La_{0.8}Th_{0.2}NbO_{4.1}$, where $a = c = 5.30$ Å, and $b = 11.58$ Å. The monoclinic angle β decreases to 90° at about the same composition and the average structure has become exactly analogous with tetragonal scheelite, remaining "locked in" at tetragonal symmetry to the high oxygen composition limit. Within the limits of error, the cell volume decreases by about 2–3% between $LaNbO_4$ and $La_{0.67}Th_{0.33}NbO_{4.165}$. A similar volume decrease has been found in the oxidation of $CeNbO_4$ to $CeNbO_{4.08}$. The $La_{0.85}Th_{0.15}NbO_{4.075}$ material underwent a second-order monoclinic to tetragonal transformation in the average structure on heating over 300°C when observed via high-temperature X-ray diffraction. This second-order transition has been observed previously for pure rare earth niobates (*12*), and all monoclinic compositions in the incommensurate phase probably exhibit this transition at elevated temperatures. The existence of the tetragonal average structure at room temperature in some of the modulated phase compositions at high oxygen excess may be a quench phenomenon. A high-temperature powder X-ray diffraction study of all these compositions has revealed a large hysteresis in the monoclinic to tetragonal inversion temperature, which is very sensitive to the previous thermal history of the specimen and to the heating/cooling rate. The phase transition on heating from mono-

clinic to tetragonal for specimens originally quenched into H_2O from 1600–1650°C varied from ~525° for the composition $La_{0.93}Th_{0.07}NbO_{4.035}$ to ~350° for $La_{0.85}Th_{0.15}NbO_{4.075}$. On cooling the reverse transition took place only ~25° lower for the first composition but 150–250°C lower for the latter. On reheating, the transition temperatures are reproducible for the first composition but 150–200° lower for all compositions with higher oxygen content. For the compositions containing 20 and 25% $ThNbO_{4.5}$, which are apparently tetragonal throughout their temperature range, one of the satellite peaks characteristic of the structural modulation (which occurs between 26 and 26.5° 2θ for Cu$K\alpha$ radiation) was observed to about 1300°C, the highest temperature examined.

A small two-phase region exists between the structurally modulated phase and another phase with a wide range of composition centered about a metal to oxygen ratio similar to that of $CeNbO_{4.25}$. The kinetics of formation of this phase are sluggish, and long annealing times close to the solidus temperature are necessary to produce single phase material. The range of composition is approximately $La_{0.59}Th_{0.41}NbO_{4.205}$–$La_{0.39}Th_{0.61}NbO_{4.305}$. Single crystals of this compound could not be obtained. The powder pattern for a composition $La_{0.45}Th_{0.55}NbO_{4.275}$ has five strongest lines at 3.198, 3.089, 2.896, 2.663, and 2.616 Å, and indicates that it may be related in structure to $CeNbO_{4.25}$. There is no specific evidence in the powder X-ray diffraction patterns that the solid solution in this phase has a modulated structure.

TABLE I

POWDER PATTERN FOR $La_{0.33}Th_{0.67}NbO_{4.33}$ ($LaTh_2Nb_3O_{13}$)

hkl	d_{calc}	d_{obs}	I/I_o
110	4.869	4.862	10
011	4.716	4.711	20
$\bar{1}21$	3.195	3.194	100
130	3.134	3.131	15
121	3.070	3.067	100
040	2.8948	2.8941	70
200	2.6834	2.6828	40
002	2.5820	2.5808	40
$\bar{1}12$	2.3309	2.3322	5
211	2.2824	2.2822	20
141	2.2609	2.2618	5
112	2.2343	2.2344	5
221	2.1600	2.1616	5
051	2.1130	2.1133	15
240	1.9680	1.9681	30
042	1.9269	1.9270	50

The third intermediate compound exhibits a range of composition, between approximately $La_{0.35}Th_{0.65}NbO_{4.325}$ and $La_{0.26}Th_{0.74}NbO_{4.37}$, which includes a composition where a compound occurs in oxidized cerium niobate, $CeNbO_{4.33}$. This compound has a powder X-ray diffraction pattern whose intensities and line positions are strongly related to those of the fergusonite-type monoclinic distortion of the scheelite structure displayed by pure $LaNbO_4$. The lattice parameters are, at $La_{0.33}Th_{0.67}NbO_{4.33}$, a = 5.375(2), b = 11.579(4), c = 5.172(2) Å, β = 93.23(4)°. There is no specific evidence in the X-ray powder diffraction patterns for the existence of superstructure in this compound, which would be evidence for ordering within the necessarily highly defective structure. The powder pattern for this material is shown in Table I. The unit cell volume is 3% smaller than the pure $LaNbO_4$.

The fourth intermediate compound occurs at $La_{0.2}Th_{0.8}NbO_{4.4}$ and does not show a significant range of solid solution. Although we did not obtain a single crystal of this material, the strong resemblance of its powder diffraction pattern to that of $ThNbO_{4.5}$ indicates that the structures must be closely related. The five strongest lines in the powder pattern occur at 4.298, 2.915, 3.223, 3.184, and 2.618 Å. A two-phase region, with no apparent solid solution, exists between $La_{0.2}Th_{0.8}NbO_{4.4}$ and the end-

member $ThNbO_{4.5}$. The solidus relationships in this portion of the diagram are complicated by the fact that $ThNbO_{4.5}$ does not melt congruently, and we therefore indicate the relationships as dashed lines in Fig. 2. In the course of this study we found it necessary to study the ThO_2–Nb_2O_5 binary system near $ThNbO_{4.5}$, which was originally reported as melting congruently (*9*). The revised ThO_2–Nb_2O_5 phase diagram and $ThNbO_{4.5}$ unit cell and powder pattern have been presented in a separate publication (*10*).

Structural Modulation

Many materials display a long-range order which can most easily be described as a sinusoidal modulation of one or more atomic coordinates in the structure about some average value (*13*). Such structural modulations involve either a fluctuation about a mean composition, or incremental displacements of atoms from their mean positions, or a combination of both. The modulations need not be purely sinusoidal, and often contain higher order harmonics. Structural modulations result in characteristic diffraction effects observable by X-ray neutron or electron diffraction, appearing as satellite reflections about the normally present Bragg reflections from the average structure (the average over all modulation).

In the most general case, the structure is modulated in three dimensions, and three characteristic basis vectors must be defined. The modulation basis vectors (in reciprocal space) p_1^*, p_2^*, p_3^*, can be resolved into components along a^*, b^*, and c^* such that the average structure coordinate system is referenced:

$$\mathbf{p}_i^* = x_i\mathbf{a}^* + y_i\mathbf{b}^* + z_i\mathbf{c}^*$$

The structural modulation is incommensurate when one or more of the $\mathbf{p}_i^*$ are not a rational fraction of an average structure reciprocal lattice vector. Each point in the reciprocal lattice of such a structure must then be represented by six indices:

$$\mathbf{r}^* = h\mathbf{a}^* + k\mathbf{b}^* + l\mathbf{c}^* + m_1\mathbf{p}_1^* + m_2\mathbf{p}_2^* + m_3\mathbf{p}_3^*,$$

where h, k, l, are the usual Miller indices, and m_1, m_2, and m_3 are similarly indices for the structural modulation. The incommensurate structural modulation in the $CeNbO_{4.08}$-type phases discussed in this paper is two dimensional in nature, and long-range ordered.

The Modulated Phase in the $LaNbO_4$–$ThNbO_{4.5}$ System

The characteristics of the modulated phase of the $CeNbO_{4.08}$ type in the $LaNbO_4$–$ThNbO_{4.5}$ system were studied in some detail, as the phase exists over a wide range of compositions. The variation of the incommensurability of the structural modu-

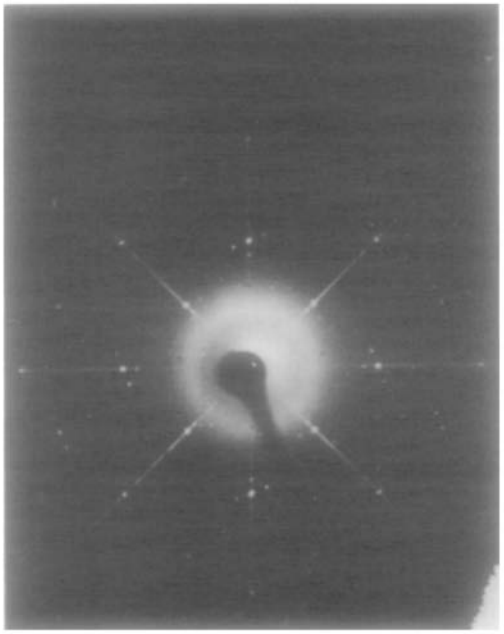

FIG. 3. Zero-level reciprocal lattice in the a^*c^* plane in $LaTh_{0.8}Nb_{0.2}O_{4.1}$: Precession method, white radiation.

lation with oxygen content was studied with both single crystal and powder X-ray diffraction data at eight excess oxygen compositions. Small single crystals for five compositions were obtained by heating powders in the solid state at temperatures just below the solidus temperatures determined by the phase equilibria studies for periods of 2 to 3 days. Crystals were removed from the furnace at the annealing temperature and cooled in air to room temperature, which occurs in 10 to 15 min. Information was obtained at three other compositions from the positions of uniquely indexable satellite reflections visible in X-ray powder diffraction patterns taken at room temperature.

An example of the diffraction effects characteristic of the modulated structures is presented in Fig. 3. This is a zero-level precession photograph of (La,Th)NbO_{4+x} ($x = 0.1$) at room temperature in an orientation where $\mathbf{b}^*$ of the monoclinic average structure is parallel to the X-ray beam and $\mathbf{a}^*\mathbf{c}^*$ of the average structure are in the plane of the film (presenting an undistorted section at the reciprocal lattice perpendicular to $\mathbf{b}^*$ at $\mathbf{b}^* = 0$). Spots characteristic of the incommensurate structural modulation form two-dimensional arrays around the average structure reflections (which are the strong spots on the radial streaks). Our studies show that the two modulation basis vectors, here called $\mathbf{p}_1^*$ and $\mathbf{p}_3^*$ to emphasize the monoclinic symmetry, do not have components parallel to $\mathbf{b}^*$ of the monoclinic average structure. Within the accuracy of the measurements, the angle between $\mathbf{p}_1^*$ and $\mathbf{p}_3^*$ is equal to β^* of the parent structure, and the lengths $|p_1^*|$ and $|p_3^*|$ are equal. The fact that the incommensurate reflections are spots and not rods (i.e., not of infinite extent parallel to $\mathbf{b}^*$) indicates that the planes of defects perpendicular to $\mathbf{b}$ are perfectly correlated with respect to each other. Higher order satellite reflections up to $m_1 = \pm 3$ can be seen in single-crystal X-ray diffraction patterns along p_1^* and up to $m_3 = \pm 2$ along $\mathbf{p}_3^*$. Intense higher-order satellite reflections may indicate the presence of higher order harmonics in the structural modulation (*14*). Satellites with both $m_1 \neq 0$ and $m_3 \neq 0$ are observed, and there are no apparent systematic absence for the satellites visible in the $b^* = 0$ level precession photographs.

Two parameter sets can be used to characterize the modulated structure and its variation with composition. In this case, the components of the modulated structure basis vectors $\mathbf{p}_i^*$ can be represented as fractions x_i and z_i of the reciprocal cell axes a^* and c^*. The variation of the components of $\mathbf{p}_i^*$ with oxygen excess for the (La,Th)NbO_{4+x} solid solution is shown in Fig. 4. The figure indicates that there are relatively large changes in x_i and z_i with initial oxygen introduction, and a decrease in the rates of change at higher oxygen contents. Although the values of x_i and z_i pass through some values which could be considered as commensurate, there is no evidence that they "lock-in" to any of these values for any appreciable range in composition. In the $LaNbO_4$–$LaWO_{4.5}$ modulated

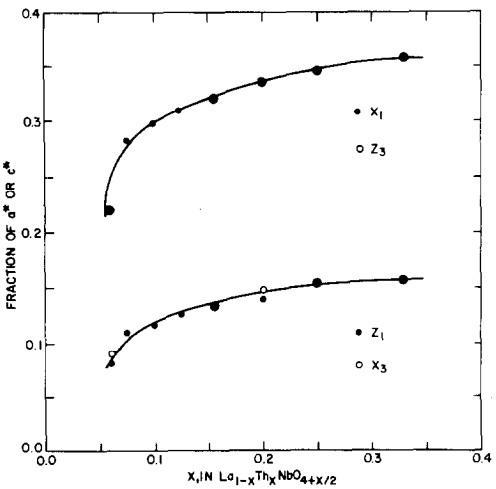

FIG. 4. Variation of reciprocal space parameters x_i and z_i in $p_i^* = x_i^* a^* + z_i c^*$.

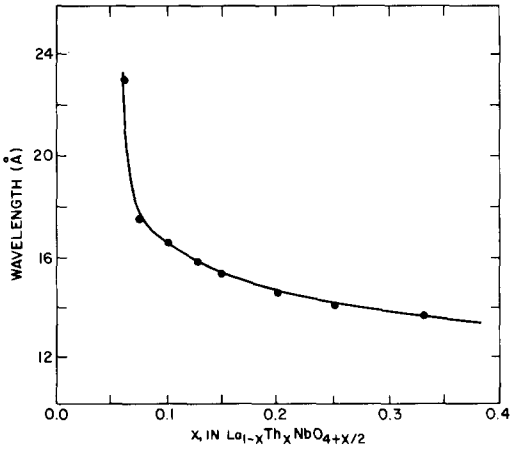

FIG. 5. Variation of the wavelength of the structural modulation with oxygen excess.

structure phase we have characterized only one composition, $LaNb_{0.79}W_{0.21}O_{4.105}$, and have found $x_1 = z_3 = 0.34$ and $x_3 = z_1 = 0.15$.

The second parameter set is related to the characteristics of the modulation in real space, and is taken as the wavelength of the modulation, given by $1/|p_1^*|$, and the angle of the plane normal to the direction of the modulation represented by p_1^* with the average structure (100) plane, obtained from the corresponding angles in reciprocal space. The variation of these parameters with oxygen excess is shown in Figs. 5 and 6. As in the reciprocal space parameters, there is a pronounced change with initial oxygen excess, and a decrease in the rate of change at higher oxygen contents. The angle between the plane normal to the direction of the modulation and the average structure (100) plane changes from 21 to 24° over the range of composition. The wavelength of the modulation varies between 23 and 13.5 Å, and, in the directions observed, is not commensurate with a repeat distance along any elementary direction in the real space lattice. The parameters describing the modulation are summarized in Table II.

We have not studied the variation of incommensurability with temperature in any detail. Heating of $LaNb_{0.8}W_{0.2}O_{4.1}$ to 400°C in a powder diffractometer did not result in any change in the modulation vectors within the accuracy of the measurements. We have not studied any of our nonstoichiometric materials below room temperature. However, a study of the magnetic susceptibility of $CeNbO_4$ and $CeNbO_{4.08}$ down to 4.2 K found no evidence for a phase transition, and confirmed the presence of Ce^{3+} and Ce^{4+} in the oxidized phase.

The determination of the exact nature of the incommensurate structural modulation would involve a study of the average structure through the measurement of the scheelite-like reflections, and a study involving the intensities of the observed incommensurate satellite reflections. This has not been done for the $CeNbO_{4.08}$-type modulated structure, but a plausible structural model can be proposed from the data available. The intensities of the satellites with respect to their associated average structure reflections clearly increase with increasing distance from the center of reciprocal space in the direction corresponding to $\mathbf{p}_1^*$, a characteristic of atomic-displacement modulation. We therefore pos-

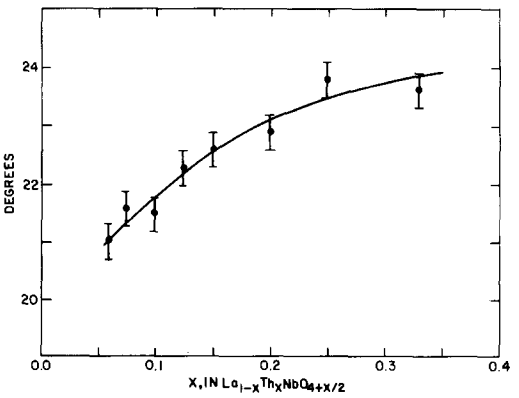

FIG. 6. Variation of the angle between the (100) plane of the average structure and the plane normal to the direction of the structural modulation with oxygen excess. Error bars are maximum deviation in the multiple measurement of the angles on precession photographs.

TABLE II

VARIATION OF INCOMMENSURABILITY IN $(La,Th)NbO_{4+z}$ WITH OXYGEN CONTENT

Compound	Data source	Vector	x	z	λ (Å)	Angle (degrees)
$La_{0.94}Th_{0.06}NbO_{4.03}$	XTL	P1	0.219	0.083	22.93(20)	21.0(3)
		P3	−0.087	0.217		
$La_{0.925}Th_{0.075}NbO_{4.0375}$	Pwdr	P1	0.284	0.111	17.48(15)	21.6(3)
$La_{0.9}Th_{0.1}NbO_{4.05}$	Pwdr	P1	0.300	0.117	16.56(15)	21.5(3)
$La_{0.875}Th_{0.125}NbO_{4.0625}$	Pwdr	P1	0.313	0.128	15.87(15)	22.3(3)
	Pwdr	P1	0.308	0.125		
$La_{0.85}Th_{0.15}NbO_{4.075}$	XTL	P1	0.320	0.132	15.34(06)	22.6(3)
		P3	−0.133	0.321		
$La_{0.8}Th_{0.2}NbO_{4.1}$	XTL	P1	0.333	0.141	14.57(10)	22.9(3)
		P3	−0.144	0.332		
$La_{0.75}Th_{0.25}NbO_{4.125}$	XTL	P1	0.344	0.152	14.10(4)	23.8(3)
		P3	−0.151	0.344		
$La_{0.67}Th_{0.33}NbO_{4.165}$	XTL	P1	0.357	0.156	13.62(20)	23.6(3)
		P3	−0.156	0.357		

tulate that the nonstoichiometry results in the occurrence of the excess oxygen in interstitial positions, causing displacements of a significant fraction of the atoms in the structure from their mean positions. Although we believe that modulation to be primarily displacive in nature, the possible presence of an accompanying compositional modulation cannot be ruled out.

The scheelite structure (*15*) consists of planes of cations alternating with two planes of anions perpendicular to **b** (in the monoclinic distortions). The two planes of anions form a puckered hexagonal close-packed array. There are four cation layers per unit cell, with the *A* and *B* cations forming interpenetrating square sublattices. There are two locations in the structure which might accommodate interstitial oxygen. Interstitial volumes of substantial size occur within the cation layers, and placement of the interstitial oxygen there would displace nearby cations. The excess oxygen might be incorporated into the existing puckered HCP oxygen planes in a manner commonly found in vernier-type nonstoichiometric compounds. Excess oxygen in these positions would displace the oxygen atoms in the structure from their normally occupied positions, and might also cause a displacement of the cations from their ideally occupied sites to accommodate changes in coordination. Both possibilities would give rise to a displacive structural modulation.

Electrical Conductivity

Conductivities were studied for the "pure" $LaNbO_4$ end-member and three compositions, $La_{0.93}Th_{0.07}NbO_{4.035}$, $La_{0.9}Th_{0.1}NbO_{4.05}$ and $La_{0.8}Th_{0.2}NbO_{4.1}$ in the modulated phase. A typical complex impedance plane plot, Fig. 7, shows a single semicircle, not seriously depressed (Δ = 3.8°), which we attribute to the geometrical capacitance of the sample. The low-frequency points indicate a nearly reversible electrode response. Such a response at the electrode is expected either for a sample conductivity which is primarily electronic, or if the porous platinum paste electrode is essentially reversible to oxygen. Transference number measurements, necessary to characterize the electronic and ionic components of the conductivity, are beyond the scope of the present study.

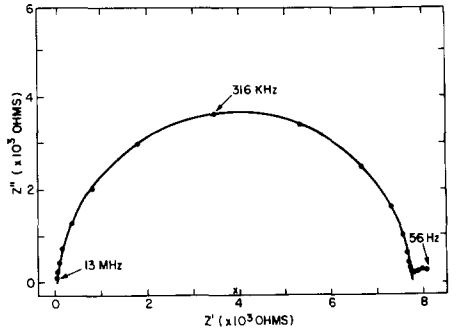

FIG. 7. Complex impedance plane plot for polycrystalline pellet of $La_{0.8}Th_{0.2}NbO_{4.1}$ at 606°C.

Plots of log σT against $1/T$ are presented in Fig. 8. The measured activation energies and conductivities at 1000°C are presented in Table III. The conductivity in $LaNbO_4$ is low and is likely to be dominated by impurities at the temperature investigated. The conductivities in the structurally modulated phase are several orders of magnitude larger than that of the end-member, but within that phase decrease with increasing oxygen content. The activation energies in the modulated phase, 1.4(1) eV, are identical within experimental error. The conductivities cannot be dominated by an unknown dopant, inadvertently added in small quantities, as that could not cause an initial large increase and then decrease in the conductivity.

If the conductivity is primarily electronic, then the concentration of mobile electronic defects in the modulated phase is apparently decreasing with increasing donor and acceptor concentrations after an initial increase over $LaNbO_4$. Once within the modulated phase, a change in the electronic conductivity might be related to changes in the periodicity of the modulation with oxygen excess. If the conductivity is primarily ionic, then the decrease in conductivity with increased oxygen excess might be due to increased association of the potential charge carriers. In either case, the strong interactions produced by the oxygen

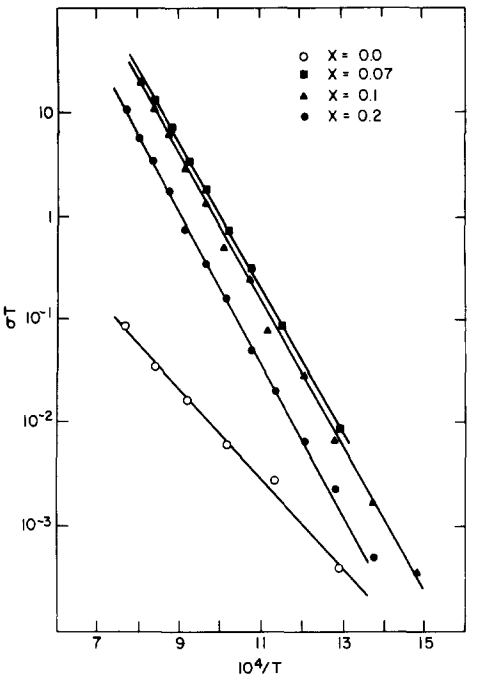

FIG. 8. Conductivity for $LaNbO_4$ and three compositions in the structurally modulated phase as a function of temperature.

excess which give rise to the structural modulation must also dominate the conductivity.

Conclusions

We have synthesized several highly defective scheelite-based compounds strongly related to the oxidized variants of $CeNbO_4$. The phase equilibria are complex, especially in the $LaNbO_4$–$ThNbO_{4.5}$ system, but

TABLE III

CONDUCTIVITY IN THE $LaNbO_4$–$ThNbO_{4.5}$ SYSTEM

Composition	σ at 1000°C (S-cm)	Activation energy (eV)
$LaNbO_4$	5.5×10^{-5}	0.85(10)
$La_{0.93}Th_{0.07}NbO_{4.035}$	2.6×10^{-2}	1.4(1)
$La_{0.9}Th_{0.1}NbO_{4.05}$	2.2×10^{-2}	1.4(1)
$La_{0.8}Th_{0.2}NbO_{4.1}$	6.8×10^{-3}	1.5(1)

they have allowed us to study the effect of anion excess in scheelite-like compounds whose temperature/oxygen partial pressure stability regions are easily accessible. Phases exhibiting incommensurate structural modulations of the scheelite structure type have been shown to exist in oxygen excess ABO_{4+x} compounds with charge compensating aliovalent cations on both the A and B sublattices. The structural modulations give rise to sharp, intense reflections in reciprocal space, and are two-dimensional in nature. In both the $LaNbO_4$–$ThNbO_{4.5}$ and $LaNbO_4$–$LaWO_{4.5}$ systems the structurally modulated phase exists over a significant range of oxygen excess, and its characteristics have been shown to be concentration dependent. The oxidized cerium compound $CeNbO_{4.08}$ also displays an incommensurate structural modulation, and may have a range of composition and incommensurability that is as yet unobserved. We have been able to produce the same type of structural modulation in $NdTaO_4$, which is also a fergusonite-type distorted scheelite, with the addition of $ThTaO_{4.5}$, and in $LaNbO_4$ doped with $LaMoO_{4.5}$. We feel that the modulated structure described here may generally occur in any scheelite based compound synthesized with a small anion excess.

A study of the specimens described in this paper has been made by A. Olsen and R. S. Roth at Arizona State University utilizing electron diffraction and high-resolution lattice image techniques. The results and structural implications of these studies will be published in the near future.

Acknowledgments

The authors have benefited greatly from conversations with A. D. Franklin and L. P. Domingues concerning various aspects of this work. J. V. Waszczak and F. J. DiSalvo made the magnetic susceptibility measurements.

References

1. R. S. Roth, T. Negas, H. S. Parker, D. B. Minor, and C. Jones, *Mater. Res. Bull.* **12,** 1173 (1977).
2. T. Negas, R. S. Roth, C. L. McDaniel, H. S. Parker, and C. D. Olson, *Mater. Res. Bull.* **12,** 1161 (1977).
3. R. J. Cava, R. S. Roth, T. Negas, and D. B. Minor, *in* "The Rare Earths in Modern Science and Technology" (G. J. McCarthy and J. J. Rhyne, Eds.), p. 181. Plenum, New York (1978).
4. R. S. Roth, *in* "The Rare Earths in Modern Science and Technology" (G. J. McCarthy and J. J. Rhyne, Eds.), p. 163. Plenum, New York (1978).
5. A. Santoro, M. Marezio, R. S. Roth, and D. B. Minor, *J. Solid State Chem.* **35,** 167 (1980).
6. M. Dvanova, G. Balagira, and E. Ya. Rode, *Inorg. Mater. (USSR),* **6,** 803 (1970).
7. A. Santoro and A. Mighell, private communication.
8. R. D. Shannon and C. T. Prewett, *Acta Crystallogr. Sect. B* **25,** 925 (1969).
9. C. Keller, *J. Inorg. Nucl. Chem.* **27,** 1236 (1965).
10. R. J. Cava, R. S. Roth, and D. B. Minor, *J. Amer. Ceram. Soc.* **64,** C-64 (1981).
11. E. P. Savchenko, N. A. Godina, and E. K. Keller, *in* "Chemistry of High Temperature Materials" (N. A. Toropov, Ed.), p. 111. Consultants Bureau, New York (1969).
12. K. Gingerich and H. Blair, *in* "Advances in X-ray Analysis," pp. 22–30. Univ. of Denver Press, Denver (1963).
13. J. M. Cowley, J. B. Cohen, M. B. Salamon, and B. J. Wuensch, Eds., "Modulated Structures—1979," AIP Conference Proceedings 53, Amer. Inst. Phys., New York (1979).
14. D. deFontaine, *in* "Local Atomic Arrangements Studied by X-Ray Diffraction" (J. B. Cohen and J. E. Hilliard, Eds.), Met. Soc. Conf., Vol. 36, pp. 51–94 (1966).
15. A. Zalkin and D. H. Templeton, *J. Chem. Phys.* **40,** 501 (1964).